RESEARCH PAPER

PCCP
www.rsc.org/pccp

Formation and decay of pyrene radical cation and pyrene dimer radical cation in the absence and presence of cyclodextrins during resonant two-photon ionization of pyrene and sodium 1-pyrene sulfonate†

Michihiro Hara, Sachiko Tojo, Kiyohiko Kawai and Tetsuro Majima*

The Institute of Scientific and Industrial Research (SANKEN), Osaka University, Mihogaoka 8-1, Ibaraki, Osaka 567-0047, Japan. E-mail: majima@sanken.osaka-u.ac.jp; Fax: Japan +6-6879-8499; Tel: Japan +6-6879-8495.

Received 5th March 2004, Accepted 23rd March 2004
First published as an Advance Article on the web 29th April 2004

Formation and decay of pyrene radical cation and pyrene dimer radical cation during resonant two-photon ionizations (TPI) of pyrene (Py) and sodium 1-pyrene sulfonate (NaPySA) in the absence and presence of cyclodextrins were studied with visible and near IR transient absorption measurement using 355-nm laser flash photolysis technique. Ionization of Py and 1-pyrene sulfonate anion ($PySA^-$) occurred within the laser flash (5 ns) to give Py radical cation ($Py^{\bullet+}$) and $PySA^-$ radical cation ($Py^{\bullet+}SA^-$) having $Py^{\bullet+}$ chromophore. Dimerizations of $Py^{\bullet+}$ and Py and of $Py^{\bullet+}SA^-$ and $PySA^-$ were observed to give the dimer radical cations ($Py_2^{\bullet+}$ and $Py_2^{\bullet+}(SA^-)_2$) based on time-resolved measurements of the charge resonance (CR) band. The TPI of $PySA^-$ was also examined in the presence of β- and γ-cyclodextrins (βCD and γCD, respectively). $Py_2^{\bullet+}(SA^-)_2$ in the cavity of two γCDs having fully overlapped structure showed the CR band around 1700 nm, while $Py_2^{\bullet+}(SA^-)_2$ in the cavity of two βCD having partially and fully overlapped structures indicated the CR bands around 1500 or 1700 nm, respectively. On the basis of formation and decay rates of $Py_2^{\bullet+}(SA^-)_2$, bimolecular formation of $Py_2^{\bullet+}(SA^-)_2$ and the neutralization are inhibited in the cavities of CDs. Selective formation of the fully overlapped structure of $Py_2^{\bullet+}(SA^-)_2$ in the cavity of two γCDs within a laser flash is explained by direct TPI of two $PySA^-$s with the parallel structure of two Py chromophores in two $PySA^-$s in the cavity of two γCDs.

Introduction

Fluorescence of pyrene (Py) has been used as a probe of environments around the Py site in micelles, macromolecules, and other materials, since both Py in the singlet excited state ($^1Py^*$) and Py excimer ($^1Py_2^*$) fluoresce in high quantum yields and show different fluorescent properties.[1–6] Time profiles of $^1Py^*$ and $^1Py_2^*$ fluorescence and the fluorescence intensity ratio indicate the interaction of two Pys in the ground and singlet excited states which informs the structure and transient behaviors of the environments. Py radical cation ($Py^{\bullet+}$) reacts with Py to give Py dimer radical cation ($Py_2^{\bullet+}$) with face-to-face structure based on the transient absorption spectra. Namely $Py^{\bullet+}$ and $Py_2^{\bullet+}$ have the characteristic absorption peaks around 450 nm[7–13] and 395 and 520 nm,[13,14] respectively, in the visible region, while $Py_2^{\bullet+}$ has the charge resonance (CR) absorption band around 1400–1700 nm in the near infrared (NIR) region in polar solvents.[8,9,14–17] Formation of $^1Py_2^*$ results from the interaction of $^1Py^*$ and Py within the lifetime of $^1Py^*$ (190–650 ns, depending on the solvents),[18–20] while $Py_2^{\bullet+}$ forms from the reaction of $Py^{\bullet+}$ and Py in the time range of 0.1–100 μs depending on the concentration of Py ($[Py] = 10^{-6}$–10^{-3} M).[13,15,21] In other words, $^1Py^*$ and $^1Py_2^*$ fluorescence provides information about the environment around the Py site in the ground state and in the singlet excited state in the time scale of 190–650 ns, while $Py^{\bullet+}$ and $Py_2^{\bullet+}$ absorption might provide information about the dynamics in the time range of 0.1–100 μs.

Absorption of $Py^{\bullet+}$ and $Py_2^{\bullet+}$ can be used to obtain the structure and transient behaviors of the environment around the Py site. Intramolecular interaction of two pyrenyl groups in Py dimer model compounds having two pyrenyl groups linked with different methylene chains is discussed based on $Py^{\bullet+}$ and $Py_2^{\bullet+}$ absorption measurements. Two types of $Py_2^{\bullet+}$ with partially (PO) and fully overlapped (FO) structures exist to have independent CR bands around 1420 and 1600 nm, respectively, as indicated by the absorption measurement of intramolecular $Py_2^{\bullet+}$ in 1,3-bis(1-pyrenyl)propane radical cation. There are various methods of kinetic study involving the formation of $Py^{\bullet+}$ such as resonant two-photon ionization (TPI),[7,11,18,22–24] photoinduced electron transfer,[12,16,25] pulse radiolysis,[13,15,21] and γ-ray radiolysis.[8,9]

Inclusion of one or two Pys in cyclodextrins (CD) results from hydrophobic interaction between Py and the inside cavity of CD,[26] while the inclusion effects on $^1Py^*$ and $^1Py_2^*$ have been studied by fluorescence enhancement.[10,27–36] Formation of Py radical anion from the reaction of $PySA^-$ and hydrated electron (e_{aq}^-) and the CD inclusion effect on the reaction have been reported during pulse radiolysis of $PySA^-$ in water in the presence of CD.[37] However, the inclusion effects on the formation and decay of $Py^{\bullet+}$ and $Py_2^{\bullet+}$ have not been reported. This study investigates the formation of $Py^{\bullet+}$ and intermolecular $Py_2^{\bullet+}$ from the TPI of Py using the transient absorption measurement in the visible and NIR region to elucidate the environmental effects such as solvent effect and inclusion effects in CD. Because of the low solubility of Py in water, sodium

---

† Electronic supplementary information (ESI) available: Kinetic traces illustrating the time profiles of ΔOD_{720} as a function of time during the TPI of NaPySA ($(2.3$–$4.3) \times 10^{-4}$ M) in the absence (no) and presence of βCD (βCD) (10^{-2} M) and γCD (γCD) (10^{-2} M) in air-saturated D_2O (Fig. 1S). See http://www.rsc.org/suppdata/cp/b4/b403409k/

DOI: 10.1039/b403409k

1-pyrene sulfonate (NaPySA) was used to study the TPI of Py included in CD. The TPI of 1-pyrene sulfonate ($PySA^-$) included in CD ($PySA^-$/CD) was examined to identify the one-electron oxidative species of $PySA^-$ ($Py^{\bullet+}SA^-$)[18,23,24] and the dimer radical cation ($Py_2^{\bullet+}(SA^-)_2$) and to elucidate the environmental effects. This study provides valuable information for understanding the effects of the environment on the one-electron oxidation of molecules.

Experimental

Materials

Py (zone refined) was purchased from Tokyo Kasei and used without further purification. NaPySA was purchased from Molecular Probe and used without further purification. β-Cyclodextrin (βCD) and γ-cyclodextrin (γCD) were purchased from Wako and purified from recrystallization. Acetonitrile (AN) with spectroscopy grade used as a solvent for the TPI was purchased from Wako and purified by drying over CaH_2 and distilling several times. 1,3-Dichloroethane (DCE), cyclohexane (CH), and D_2O were purchased from Nacalai Tesque.

Laser photolysis measurements

A flash at 355 nm (5 ns-FWHM, 100 mJ $pulse^{-1}$, diameter 1.0 cm) was obtained by the third-harmonic oscillation from a Nd^{3+}:YAG laser (Continuum Surelite). The probe beam was obtained from a 450 W Xe lamp (Osram XBO-450) synchronized using the laser flash. The detection system consisted of a photomultiplier (PMT) (Hamamatsu R928), monochromator (Nikon G250) to detect the time profiles and multichannel detector (Hamamatsu C4560-000G) to detect the spectra and a pin photodiode (Thorlabs PDA255) for the transient absorption in the NIR region. The signal from PMT was recorded on a transient digitizer (Tektronix, TSD380P). The signals were converted to transient optical densities. The laser power was measured by a laser power meter (Ophir AN/2).

The concentration of absorbed photon ([photon]) was determined from the equation, $[\text{photon}] = N_{ABS}/V_{ir} = (I_0 - I)/E_{355}Cr$, where N_{ABS} is a number of absorbed photons of a molecule in the irradiated (monitored) volume (V_{ir}). N_{ABS} is calculated from $(I_0 - I)/E_{355}$ in which I_0, I, and E_{355} are initial irradiation energy, transmitted energy, and a photon energy at 355 nm (377 kJ $einstein^{-1}$), respectively. $I_0 = 20$–100 and $I = 1$–20 mJ $pulse^{-1}$ were directly measured using a power meter (Ophir AN/2). $V_{ir} = 0.151\ cm^3$ is obtained from the cross section ($C = \pi 0.385^2 = 0.462\ cm^2$) multiplied by the width of monitor light (0.325 cm).

Results and discussion

Formation of $Py^{\bullet+}$ and $Py_2^{\bullet+}$ during TPI of Py in acetonitrile

A transient absorption spectrum with a peak at 450 nm, assigned to $Py^{\bullet+}$, was observed at 1 μs after the 355-nm laser flash during the laser flash photolysis of Py in air-saturated AN (Fig. 1). [Py] was 10^{-3} M, and absorbance at 355 nm was 1.0. The TPI of Py in AN has already been determined with excitation at 337 (ref. 18), 347 (ref. 23) and 351 nm (ref. 24), and confirmed based on the relation between the yield of $Py^{\bullet+}$ and laser power. The TPI of Py with excitation at 347 nm in AN was also reported based on photoconductivity measurement.[38] Ionization potential (IP) of phenothiazine has been reported to be 7.6 eV (ref. 39) and the decrease of IP due to the solvation effect in AN is estimated to be 1.5 eV. Since a similar solvation effect on the IP of Py (IP = 7.41 eV = 718 kJ M^{-1})[20] can be expected, the IP of Py in AN is estimated to be 5.9 eV. Therefore, the 355-nm photon energy (3.5 eV = 337 kJ $einstein^{-1}$) is not sufficient to ionize Py. The TPI of Py occurs to give $Py^{\bullet+}$ and electron under the present irradiation conditions with laser power of 56 mJ $pulse^{-1}$ and laser fluence of 120 mJ $pulse^{-1}$ cm^{-2}. From the optical density at 450 nm, $\Delta OD_{450} = 0.045$ and molar absorption coefficient of $Py^{\bullet+}$ at 443 nm ($\varepsilon_{443} = 11\,400\ M^{-1}\ cm^{-1}$)[12] [$Py^{\bullet+}$] was calculated to be 4.0×10^{-6} M. The quantum yield of ionization (Φ_{ion}) of Py was calculated to be 2.7×10^{-4} (Table 1).

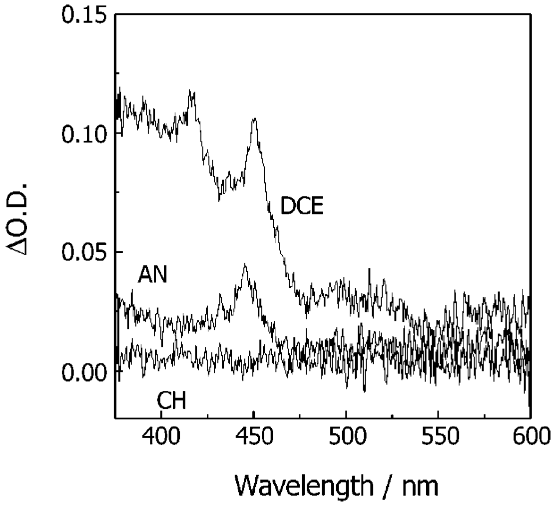

Fig. 1 Transient absorption spectra of $Py^{\bullet+}$ observed at 1 μs after a flash during the TPI of Py at the concentrations of 3.0×10^{-3}, 2.4×10^{-3}, and 3.7×10^{-3} M in air-saturated 1,2-dichloroethane (DCE), acetonitrile (AN), and cyclohexane (CH).

Transient absorption measurement in the NIR region was performed during the TPI of Py in AN. A transient absorption spectrum with a broad band around 1500 nm was observed immediately after the laser flash and assigned to the dimer radical anion of AN ($AN_2^{\bullet-}$) according to that observed during the pulse radiolysis of AN.[41] Both $\Delta OD_{455}(Py^{\bullet+})$ and ΔOD_{1500} ($AN_2^{\bullet-}$) decreased in the time scale of 1 μs after the flash through the charge recombination. The concentration of $AN_2^{\bullet-}$ at 1 μs after a laser flash was calculated to be 5×10^{-7} M based on the molar absorption coefficient at 1450 nm ($\varepsilon_{1450} = 23\,000\ M^{-1}\ cm^{-1}$).[41] The lower concentration of $AN_2^{\bullet-}$ than that of $Py^{\bullet+}$ is probably attributed to the quenching of $AN_2^{\bullet-}$ by oxygen saturated in AN solvent.

Solvent effects on the formation of $Py^{\bullet+}$ and $Py_2^{\bullet+}$ during TPI of Py

The solvent effects on the TPI of Py were examined. A large value of $\Delta OD_{450} = 0.11$ was observed in air-saturated DCE. In addition, peaks around 390 and 520 nm were observed assigned to the local excitation (LE) band of $Py_2^{\bullet+}$. However, absorption at 450 nm was not observed in air-saturated CH. Fig. 2 shows the NIR transient absorption spectra observed at 5, 15, and 75 μs after a 355-nm laser flash during the TPI of Py in DCE. A large absorption band around 1500 nm was ascribed to the CR band of $Py_2^{\bullet+}$.

Charge recombination between radical cation and anion in the solvent cage occurs competitively with the dissociation to free radical ions.[42–44] The charge recombination of $Py^{\bullet+}$ and $AN^{\bullet-}$ or $AN_2^{\bullet-}$ in the solvent cage occurs at the rate of 10^8–$10^{10}\ s^{-1}$ in AN, competitively with the dissociation to free radical ions.[44] The charge recombination occurs between $Py^{\bullet+}$ and electron much faster than the dissociation process in CH, the transient absorption of $Py^{\bullet+}$ was not observed during the TPI of Py using ns-laser flash. Since chloride ion (Cl^-) and 2-chloroethyl radical were generated from the dissociative electron capture of DCE, charge recombination does not occur in DCE. Since the reaction of $Py^{\bullet+}$ and Cl^- occurs at the rate

Table 1 Transient absorption of $Py^{\bullet+}$ and $Py^{\bullet+}SA^-$ ($M^{\bullet+}$) and the dimer radical cation ($M_2^{\bullet+}$) in AN and D_2O observed at 1 μs after a flash during the TPI of Py and $PySA^-$

Py or $PySA^-$	Additive	Solvent	ΔOD_{455}/ ΔOD_{1700}	$\varepsilon_{455}/\varepsilon_{1700}$/ 10^4 M^{-1} cm^{-1}	[Photons]/ 10^{-4} M	$[M^{\bullet+}]/[M_2^{\bullet+}]$/ 10^{-6} M	$\Phi_{ion}[M^{\bullet+}]$/ $\Phi_{ion}[M_2^{\bullet+}]/10^{-4}$
Py	no	AN	0.045/0[a]	1.1/0	14.4	4.0/0	2.7/0
$PySA^-$	no	D_2O	1.09/0	14.1/0	8.4	7.7/0	9.0/0
$PySA^-$	βCD	D_2O	0.92/0	15.4/0	7.4	6.0/0	8.1/0
$PySA^-$	γCD	D_2O	0.25/0.068	14.1/3.0	5.9	1.8/2.2	3.0/3.8

[a] No absorption of $M_2^{\bullet+}$ was observed at 1700 nm at 1 μs after a flash, although the transient absorption of the dimer radical anion of AN ($AN_2^{\bullet-}$) was observed around 1500 nm immediately after the laser flash.

constant of 9.4×10^9 M^{-1} s^{-1},[36] the reaction rate is calculated to be 10^4 s^{-1} at $[Cl^-] = 10^{-5}$ M and considerably slower than the charge recombination. Therefore, charge recombination is strongly prevented in DCE compared with that in acetonitrile, resulting in the higher yield of $Py^{\bullet+}$ in DCE. Formation of $Py^{\bullet+}$ in a higher concentration is followed by formation of $Py_2^{\bullet+}$ at high [Py] in DCE.

The inset shows a kinetic trace illustrating the time profile of ΔOD_{1550} as a function of time during the TPI of Py (3.0×10^{-3} M) in DCE. The absorption peak at 1500–1600 nm increased in the time scale of a few hundred ns with a half-lifetime ($\tau_{1/2}$) of 51 ns ($[Py] = 3.0 \times 10^{-3}$ M) (Fig. 2).

Since the formation of $Py_2^{\bullet+}$ occurred within 500 ns after a laser flash, the equilibrium between $Py^{\bullet+}$ and $Py_2^{\bullet+}$ was almost attained in the time scale of 500 ns. Therefore, the transient absorptions of $Py^{\bullet+}$ and $Py_2^{\bullet+}$ did not change apparently in the μs time scale (Fig. 2, inset), but decayed in the longer time scale through the neutralization.

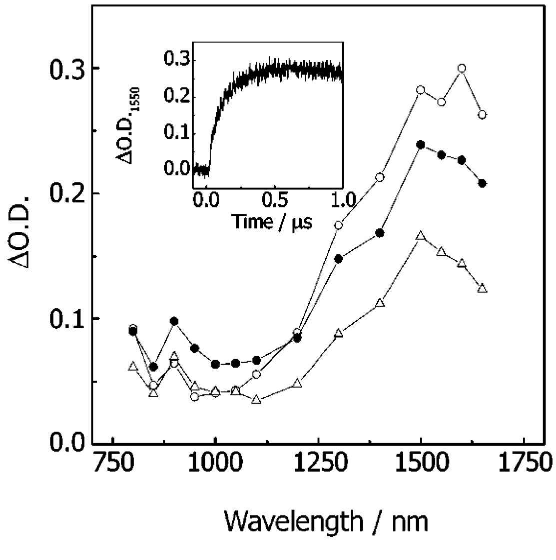

Fig. 2 Transient absorption spectra of $Py_2^{\bullet+}$ observed at 5 (○), 15(●), and 75 μs (△) after a flash during the TPI of Py (3.0×10^{-3} M) in DCE. The inset shows the growth of ΔOD monitored at 1550 nm.

Inclusion of $PySA^-$ in CDs

In order to study the TPI of Py in air-saturated water and in CD, NaPySA was used because of its high solubility in water. NaPySA exists as $PySA^-$ in water. Absorption and fluorescence spectra with peaks at 375 and 396 nm, respectively, were observed for NaPySA (2.7×10^{-4} M) in D_2O, as shown in Fig. 3. D_2O was used as the solvent for the absorption measurement in the NIR region. The spectra were similar to those of Py in AN.

The absorption peak of $PySA^-$ in the presence of βCD and γCD shifted slightly to the longer wavelength region because of the inclusion of $PySA^-$ in the ground state in βCD and γCD.[34–36] The association constant of 1:1-inclusion compound between $PySA^-$ and βCD ($PySA^-$/βCD) was found to be 30 M^{-1} by Harada *et al.*[35] The absorption spectrum of $PySA^-$ included in γCD showed peaks at around 375 nm, and the fluorescence spectrum showed peaks at 396 and 486 nm. Two peaks at 396 and 486 nm in the fluorescence spectra were assigned to $PySA^-$ in the singlet excited state ($^1PySA^{-*}$) and the excimer, respectively. Since dimerization of $PySA^-$ does not occur under the experimental conditions, the excimer emission is responsible to two $PySA^-$s included in the cavity of γCD.

It has been reported that two $PySA^-$s are included in the cavity of two γCDs to give 2:2-inclusion compound ($(PySA^-)_2/(\gamma CD)_2$).[37,40] The association constant of $PySA^-$ and γCD giving 1:1-inclusion compound ($PySA^-/\gamma CD$) has been found to be 1 M^{-1}.[35] Those of $PySA^-/\gamma CD$ and $PySA^-$ giving 2:1-inclusion compound ($(PySA^-)_2/\gamma CD$), and of $(PySA^-)_2/\gamma CD$ and γCD giving 2:2-inclusion compound ($(PySA^-)_2/(\gamma CD)_2$) have been reported to be 10^6 and 2.0×10^4 M^{-1}, respectively.[35] It is suggested that $PySA^-/\gamma CD$ is formed sequentially to give $(PySA^-)_2/(\gamma CD)_2$ in 100% yield under the present experimental conditions.

Formation of $Py^{\bullet+}SA^-$ and $Py_2^{\bullet+}(SA^-)_2$ during TPI of $PySA^-$ in the absence and presence of CD

The occurrence of the TPI of $PySA^-$ is reasonably considered with the 355-nm excitation of $PySA^-$ in water in the absence and presence of CD, since the properties of $PySA^-$ are similar

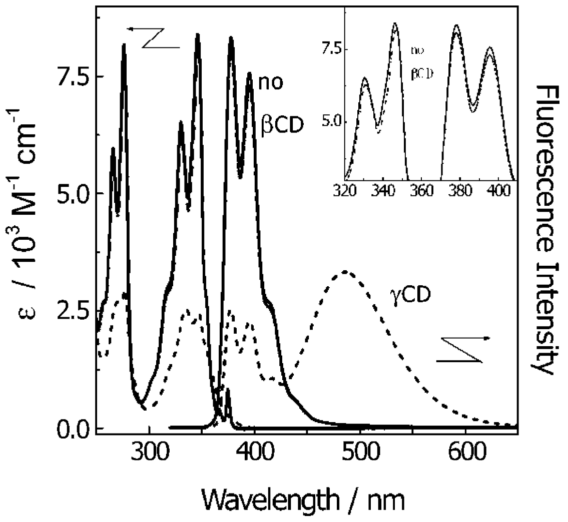

Fig. 3 Absorption and fluorescence spectra of $PySA^-$ ($[NaPySA] = 2.7 \times 10^{-4}$, 2.3×10^{-4}, and 4.3×10^{-4} M in the absence (solid line) and presence of βCD (dashed line) (10^{-2} M) and γCD (dotted line) (10^{-2} M) in D_2O. Both spectra in the absence and presence of βCD shifted slightly to the longer wavelength region. Inset: expansion of absorption and fluorescence peaks by solid and dashed lines in the region of 320–410 nm.

to those of the Py in AN. A transient absorption spectrum with a peak at 456 nm was observed at 1 μs after a laser flash during the laser flash photolysis of NaPySA (2.7×10^{-4}, 2.3×10^{-4}, and 4.3×10^{-4} M) in D_2O in the absence and presence of βCD (10^{-2} M) or γCD (10^{-2} M), as shown in Fig. 4. Absorbance of NaPySA at 355 nm was 1.0. The spectrum is almost identical to $Py^{\bullet+}$ although the peak shifted to a 10-nm longer wavelength than that of $Py^{\bullet+}$. This result indicates that the TPI of $PySA^-$/CD occurs to give $Py^{\bullet+}SA^-$/CD with $Py^{\bullet+}$-chromophore and solvated electron under the irradiation conditions at a laser power of 100 mJ and laser fluence of 215 mJ $pulse^{-1}$ cm^{-2}. The transient absorption of solvated electron in D_2O was observed at 720 nm (supporting information).† Since one-electron oxidation of the Py chromophore in $PySA^-$ occurs during the TPI of $PySA^-$,[23,24] $Py^{\bullet+}SA^-$ has positive and negative charges on the Py site and sulfonate group, respectively.[23] In other words, $Py^{\bullet+}SA^-$ is $Py^{\bullet+}$ substituted by a sulfonate group (SA^-) and it has an absorption peak at 10-nm longer wavelength compared with $Py^{\bullet+}$ because of the substituent.

Since the relation between the IP of $PySA^-$ is approximately equal to that of Py (7.41 eV)[20] and 355-nm photon energy (3.5 eV), the TPI must proceed *via* two-step two-photon excitation through $^1PySA^{-*}$ with the lifetime of 64–90 ns in water.[18,28,29]

In order to determine [$Py^{\bullet+}SA^-$] formed from the TPI, that of e_{aq}^- was calculated from the characteristic absorption peak at 720 nm which was not shown in Fig. 4. From $\Delta OD_{720} = 0.143$ at 500 ns after the laser flash ($t = 500$ ns) (supporting information)† and absorption coefficient of e_{aq}^- at 720 nm ($\varepsilon_{720} = 1.85 \times 10^4$ M^{-1} cm^{-1})[40] [e_{aq}^-] and $Py^{\bullet+}SA^-$ were calculated to be 7.7×10^{-6} M in the absence of CD. Similarly [e_{aq}] was calculated to be 6.0×10^{-6} and 4.0×10^{-6} M from ΔOD_{720} of e_{aq}^-, 0.111 and 0.074 at $t = 500$ ns, during the TPI in the presence of βCD and γCD, respectively, in D_2O. ΔOD_{455} of $Py^{\bullet+}SA^-$ in the absence and presence of βCD and γCD in D_2O were 1.09, 0.92, and 0.25 at $t = 500$ ns, respectively (Fig. 5). Therefore, ε_{455} of $Py^{\bullet+}SA^-$ was 1.41 and 1.54×10^5 M^{-1} cm^{-1} for free $Py^{\bullet+}SA^-$ and $Py^{\bullet+}SA^-$ included in βCD ($Py^{\bullet+}SA^-$/βCD), respectively, which are one-order of magnitude larger than that of $Py^{\bullet+}$ in AN ($\varepsilon_{443} = 1.14 \times 10^4$ M^{-1} cm^{-1}).[12]

Similarly to the characteristic absorption peaks of $Py_2^{\bullet+}$ around 395 and 520 nm (LE band)[13,14] around 1400–1700 nm (CR band) in polar solvents,[8,9,14–17] $Py_2^{\bullet+}$ $(SA^-)_2$ with two peaks at 395 and 520 nm and CR band around 1300–1800 nm was observed immediately after a laser flash during the TPI of $(PySA^-)_2/(\gamma CD)_2$ between two $PySA^-$s and two γCDs, but not during the TPI of $PySA^-$ in the presence of βCD. [e_{aq}^-] of 4.01×10^{-6} M equals the summation of [$Py^{\bullet+}SA^-$] and [$Py_2^{\bullet+}(SA^-)_2$]. Since ΔOD_{455} is assigned to free $Py^{\bullet+}SA^-$, [$Py^{\bullet+}SA^-$] was calculated from ε_{455} of 1.41×10^5 M^{-1} cm^{-1} to be 1.78×10^{-6} M. Therefore, [$Py_2^{\bullet+}(SA^-)_2$] was 2.23×10^{-6} M. In addition, we can estimate ε_{1700} of $Py_2^{\bullet+}(SA^-)_2$ to be 3.0×10^4 M^{-1} cm^{-1} from $\Delta OD_{1700} = 0.068$ 0.068 at $t = 500$ ns and [$Py_2^{\bullet+}(SA^-)_2$] $= 2.23 \times 10^{-6}$ M. Thus, Φ_{ion} of $Py^{\bullet+}SA^-$ during the TPI of $PySA^-$ in the absence and presence of βCD and γCD in D_2O were determined to be 9.0×10^{-4}, 8.1×10^{-4}, 3.0×10^{-4}, respectively. The Φ_{ion} of $Py_2^{\bullet+}(SA^-)_2$ during the TPI of $(PySA^-)_2/(\gamma CD)_2$ in D_2O was 3.8×10^{-4} (Table 1). This is consistent with the ratio of 1.8:2.2 for [$Py^{\bullet+}SA^-$]:[$Py_2^{\bullet+}(SA^-)_2$]. It is suggested that $PySA^-$ and $(PySA^-)_2/(\gamma CD)_2$ exist in the similar ratio under the experimental condition, and that the $Py_2^{\bullet+}(SA^-)_2$ is directly generated by the TPI of $(PySA^-)_2$ in the ground state.

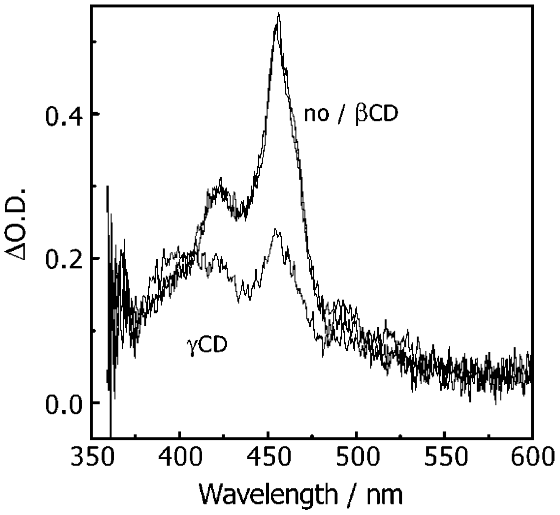

Fig. 4 Transient absorption spectra of $Py^{\bullet+}SA^-$ observed at 1 μs after a flash during the TPI of NaPySA (2.7×10^{-4}, 2.3×10^{-4}, and 4.3×10^{-4} M) in the absence and presence of βCD (10^{-2} M) and γCD (10^{-2} M) in D_2O. The spectra in the absence and presence of βCD were overlapped each other.

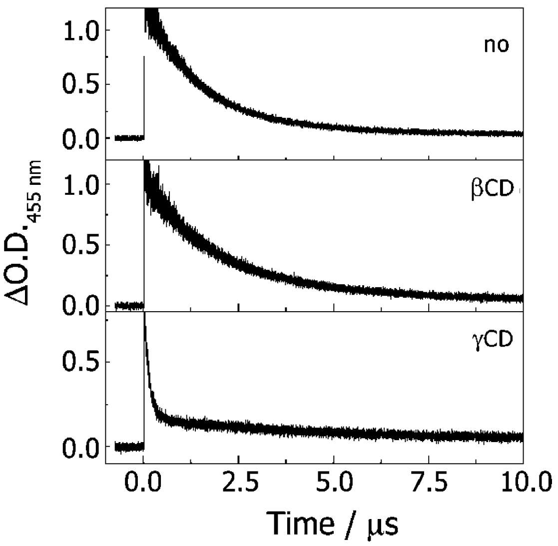

Fig. 5 Kinetic traces illustrating the time profiles of ΔOD_{455} as a function of time during the TPI of NaPySA (2.7×10^{-4}, 2.3×10^{-4}, and 4.3×10^{-4} M) in the absence (no) and presence of βCD (βCD) (10^{-2} M) and γCD (γCD) (10^{-2} M) in air-saturated D_2O. The time profiles at 100–200 ns after the laser flash were overlapped with absorptions of $Py^{\bullet+}SA^-$ and $PySA^-$ in the triplet excited state, and fluorescence of $PySA^-$.

Effects of the CD environment on the formation and decay of $Py_2^{\bullet+}(SA^-)_2$ included in CDs

Fig. 6 shows kinetic traces illustrating the time profile of ΔOD_{1700} as a function of time in the TPI of NaPySA (2.7×10^{-4}, 2.3×10^{-4}, and 4.3×10^{-4} M) in the absence and presence of βCD (10^{-2} M) and γCD (10^{-2} M) in D_2O, respectively. The absorption band around 1400–1700 nm increased in the time scale of a few μs with $\tau_{1/2}$ of 1.4 μs in the absence of CD ([NaPySA] $= 2.7 \times 10^{-4}$ M) (Fig. 6). The peaks at 1500 and 1700 nm were observed in the presence of βCD, and increased in the time scale of a few μs with $\tau_{1/2}$ of 1.8 μs ([NaPySA] $= 2.3 \times 10^{-4}$ M). The peak in the presence of γCD was observed at 1700 nm at the end of the laser pulse ([NaPySA] $= 4.3 \times 10^{-4}$ M). The peaks were assigned to the CR band of $Py_2^{\bullet+}(SA^-)_2$ in which two Py chromophores interact with each other to give a face-to-face $Py_2^{\bullet+}$. The formation lifetimes ($\tau_{1/2}$) of $Py_2^{\bullet+}(SA^-)_2$ with 1.4 μs and 1.8 μs were consistent with those of the $Py^{\bullet+}SA^-$ decay in the absence and presence of βCD, respectively (Fig. 5). Decreasing the

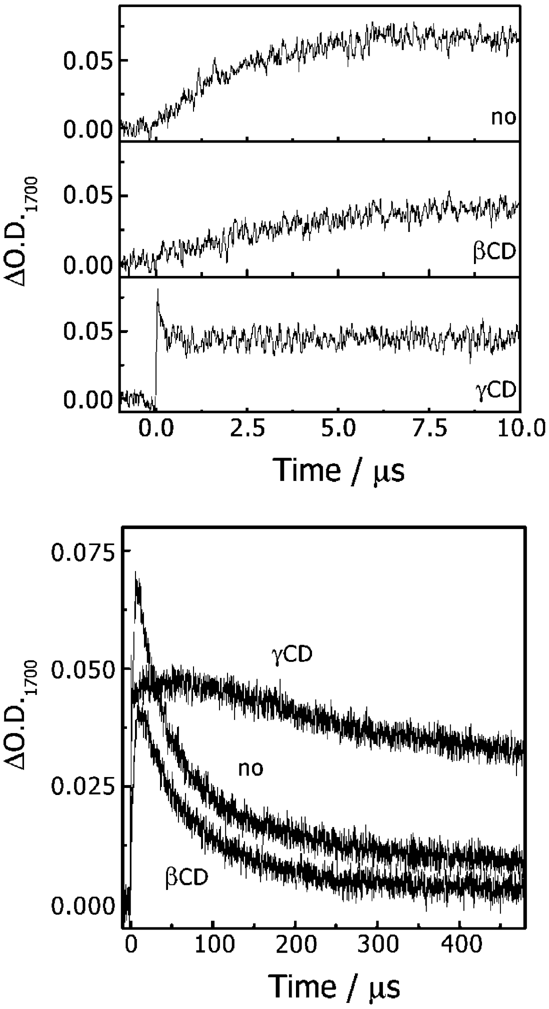

Fig. 6 Kinetic traces illustrating the time profiles of ΔOD_{1700} as a function of time during the TPI of NaPySA (2.7×10^{-4}, 2.3×10^{-4}, and 4.3×10^{-4} M) in the absence (no) and presence of βCD (βCD) (10^{-2} M) and γCD (γCD) (10^{-2} M) in air-saturated D_2O.

formation rate of $Py_2^{\bullet+}(SA^-)_2$ included in βCDs ($Py_2^{\bullet+}$-$(SA^-)_2/(\beta CD)_2$) compared with that in water is explained by steric hindrance in the cavity of βCD for the reaction of $Py^{\bullet+}SA^-$ and $PySA^-$.

Decay of $Py_2^{\bullet+}(SA^-)_2$ occurred with $\tau_{1/2}$ of 40 μs in water, while $Py_2^{\bullet+}(SA^-)_2/(\beta CD)_2$ decayed slower with $\tau_{1/2}$ of 58 μs. On the other hand, decay of $Py_2^{\bullet+}(SA^-)_2/(\gamma CD)_2$ showed two components with $\tau_{1/2}$ shorter than 1 μs and longer than 500 μs. The faster decay may correspond to the charge recombination of $Py_2^{\bullet+}(SA^-)_2/(\gamma CD)_2$ and e_{aq}^-. The slower decay of $Py_2^{\bullet+}(SA^-)_2/(CD)_2$ corresponding to the neutralization of $Py_2^{\bullet+}(SA^-)_2$ is inhibited in the cavities of βCD and γCD. Since the absorption of $Py^{\bullet+}SA^-/(\beta CD)$ and $Py_2^{\bullet+}(SA^-)_2/(CD)_2$ decayed without any change of the absorption peaks, they are stable in the time scale of 10–100 μs. No exclusion of $Py^{\bullet+}SA^-$ and $Py_2^{\bullet+}(SA^-)_2$ occurs from the cavities of βCD and CDs, respectively.

The transient absorption spectra in the NIR region were observed during the TPI of $PySA^-$ in D_2O (Fig. 7). The broad transient absorption of $Py_2^{\bullet+}(SA^-)_2$ was observed at 1400–1700 nm in D_2O, while the peak at 1700 nm was for $Py_2^{\bullet+}(SA^-)_2/(\gamma CD)_2$, and the two peaks at 1500 and 1700 nm were for $Py_2^{\bullet+}(SA^-)_2/(\beta CD)_2$. The peak must reflect partially (PO) or fully overlapped (FO) structure of $Py_2^{\bullet+}$ with the CR bands around 1500 or 1700 nm, respectively, according to the assignment of absorption peaks of intramolecular $Py_2^{\bullet+}$ in 1,3-bis(1-pyrenyl)propane radical cation with PO and FO structures around 1420 and 1600 nm, respectively.[14,17] The CR bands of $Py_2^{\bullet+}$ in $Py_2^{\bullet+}(SA^-)_2/(CD)_2$ changed in the shape and shifted to 100–150 nm longer wavelengths compared with that of $Py_2^{\bullet+}$ in $Py_2^{\bullet+}(SA^-)_2$. This difference is explained by the effect of the CD environment. Similarly, the 80–100 nm longer wavelength shifts were observed for PO and FO structure of $Py_2^{\bullet+}(SA^-)_2/(\gamma CD)_2$ compared with those of $Py_2^{\bullet+}$ in 1,3-bis(1-pyrenyl)propane radical cation.[14,17] This difference can also be explained by the effect of the CD environment and the difference of the inter- and intra-molecular $Py_2^{\bullet+}$ formation.

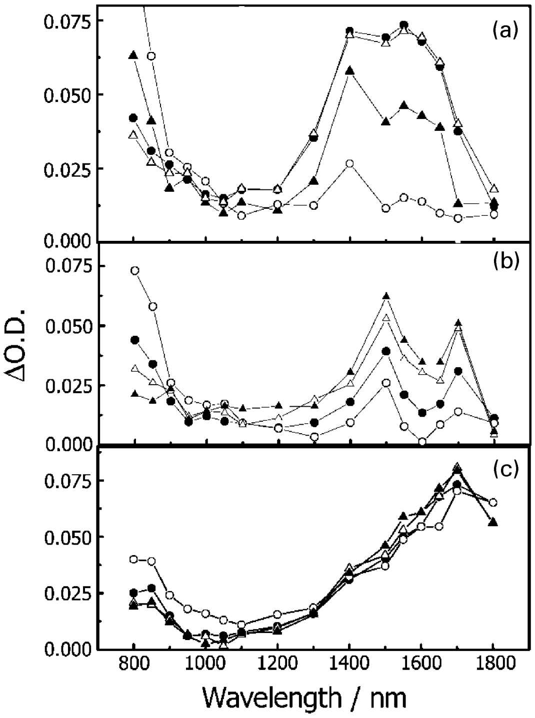

Fig. 7 Transient absorption spectra observed during the TPI of NaPySA (2.7×10^{-4}, 2.3×10^{-4}, and 4.3×10^{-4} M) in the absence (a) and presence of βCD (10^{-2} M) (b) and γCD (10^{-2} M) (c) in D_2O. Spectra measured at 0.5(○), 2 (●), 5 (△), and 10 μs (▲) after the 355-nm laser flash.

Interestingly, $Py_2^{\bullet+}$ has FO structure in $Py_2^{\bullet+}(SA^-)_2/(\gamma CD)_2$ and both PO and FO structures in $Py_2^{\bullet+}(SA^-)_2/(\beta CD)_2$. The FO structure of $Py_2^{\bullet+}$ in $Py_2^{\bullet+}(SA^-)_2/(\gamma CD)_2$ can be explained by the parallel structure of two Py chromophores in $(PySA^-)_2/(\gamma CD)_2$. Since the Py chromophore of $PySA^-$ has a larger size than the cavity of βCD, part of Py chromophore of $PySA^-$ is excluded from the cavity. Thus, $Py_2^{\bullet+}(SA^-)_2/(\beta CD)_2$ is generated by the dimerization of $Py^{\bullet+}SA^-/\beta CD$ and $PySA^-/\beta CD$ and has PO and FO structures in the cavity of two βCDs (Scheme 1). This is the first

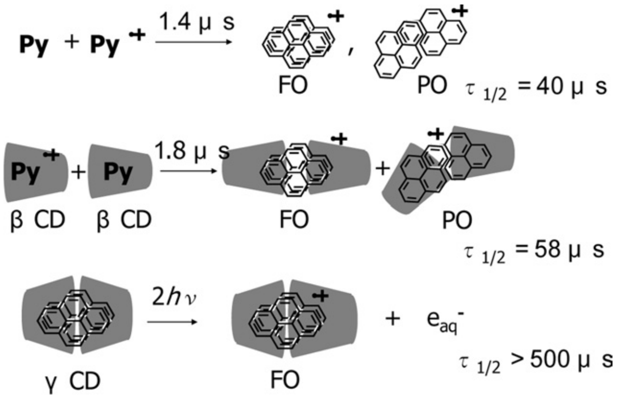

Scheme 1

observation of the kinetic formation of $Py_2^{\bullet+}(SA^-)_2/(\beta CD)_2$ from the dimerization of $Py^{\bullet+}SA^-/\beta CD$ and $PySA^-/\beta CD$. There are possibilities of the kinetic formation of $Py_2^{\bullet+}$ and $Py_2^{\bullet+}(SA^-)_2$ as a kinetic probe of the environment of the Py chromophore.

Conclusions

Formation and decay of $Py^{\bullet+}$, $Py^{\bullet+}SA^-$, $Py_2^{\bullet+}$, and $Py_2^{\bullet+}(SA^-)_2$ during the 355-nm TPI of Py and sodium $PySA^-$ in the absence and presence of cyclodextrins were investigated with the transient absorption measurement concerning the solvent effect and environment effect of the inclusion compounds of $PySA^-$ in CD. Formation and decay of $Py^{\bullet+}$, $Py^{\bullet+}SA^-$, $Py_2^{\bullet+}$, and $Py_2^{\bullet+}(SA^-)_2$ are discussed based on the LE band of the radical cations ($Py^{\bullet+}$ and $Py^{\bullet+}SA^-$) and dimer radical cations ($Py_2^{\bullet+}$ and $Py_2^{\bullet+}(SA^-)_2$) as well as the CR band of $Py_2^{\bullet+}$ and $Py_2^{\bullet+}(SA^-)_2$. Formation of $Py^{\bullet+}$ was observed in polar solvents but not in CH because of the fast charge recombination. $Py_2^{\bullet+}$ formed from dimerization of $Py^{\bullet+}$ and Py (3.0×10^{-3} M) with $\tau_{1/2}$ of 51 ns in DCE. $Py_2^{\bullet+}(SA^-)_2$ formed from dimerization of $Py^{\bullet+}SA^-$ and $PySA^-$ (2.7×10^{-4} M) with $\tau_{1/2}$ of 1.4 μs in D_2O. On the other hand, $Py_2^{\bullet+}(SA^-)_2/(\beta CD)_2$ with PO and FO structures of $Py_2^{\bullet+}$ in the cavity of two βCDs formed with $\tau_{1/2}$ of 1.8 μs at $[PySA^-] = 2.7 \times 10^{-4}$ M and $[\beta CD] = 10^{-2}$ M. $Py_2^{\bullet+}(SA^-)_2/(\gamma CD)_2$ with FO structure of $Py_2^{\bullet+}$ formed immediately after the laser flash. The PO and FO structures were identified by the characteristic CR bands around 1500 and 1700 nm, respectively. It should be emphasized that $Py_2^{\bullet+}(SA^-)_2/(\beta CD)_2$ forms from dimerization of $Py^{\bullet+}SA^-/\beta CD$ and $PySA^-/\beta CD$, while $Py_2^{\bullet+}(SA^-)_2/(\gamma CD)_2$ forms directly from the TPI of $(PySA^-)_2$ in $(PySA^-)_2/(\gamma CD)_2$. This is explained by the existence of $PySA^-/\beta CD$ and $(PySA^-)_2/(\gamma CD)_2$ in the ground state. One Py chromophore exists in the cavity of βCD, while two Py chromophores exist with the parallel configuration in the cavity of two γCDs. The neutralization of $Py_2^{\bullet+}(SA^-)_2$ is inhibited in the cavities of βCD and γCD. No exclusion of $Py^{\bullet+}SA^-$ and $Py_2^{\bullet+}(SA^-)_2$ occurs from the cavities of CD.

Acknowledgements

This work has been partly supported by a Grant-in-Aid for Scientific Research on Priority Area (417), 21st Century COE Research, and others from the Ministry of Education, Culture, Sports, Science and Technology (MEXT) of the Japanese Government.

References

1 J. Duhamel, A. Yekta and M. A. Winnik, *J. Phys. Chem.*, 1993, **97**, 2759.
2 F. M. Winnik, *Chem. Rev.*, 1993, **93**, 587.
3 M. R. Jarvis and E. W. Voss, *Mol. Immunol.*, 1981, **18**, 261.
4 Y. Inai, M. Sisido and Y. Imanishi, *J. Phys. Chem.*, 1990, **94**, 8365.
5 R. Goedeweeck, M. Vanderauweraer and F. C. Deschryver, *J. Am. Chem. Soc.*, 1985, **107**, 2334.
6 C. Garcia-Echeverria, *J. Am. Chem. Soc.*, 1994, **116**, 6031.
7 J. T. Richards, G. West and J. K. Thomas, *J. Phys. Chem.*, 1970, **74**, 4137.
8 A. Kira, M. Imamura and T. Shida, *J. Phys. Chem.*, 1976, **80**, 1445.
9 A. Kira and M. Imamura, *J. Phys. Chem.*, 1979, **83**, 2267.
10 S. Neumann, R. Korenstein, Y. Barenholz and M. Ottolenghi, *Isr. J. Chem.*, 1982, **22**, 125.
11 A. Liu, M. C. Sauer, Jr., D. M. Loffredo and A. D. Trifunac, *J. Photochem. Photobiol., A*, 1992, **67**, 197.
12 A. Tsuchida, M. Yamamoto and Y. Nishijima, *J. Phys. Chem.*, 1984, **88**, 5062.
13 A. Kira, S. Arai and M. Imamura, *J. Chem. Phys.*, 1971, **54**, 4890.
14 A. Tsuchida, Y. Tsujii, M. Ohoka and M. Yamamoto, *J. Phys. Chem.*, 1991, **95**, 5797.
15 M. A. J. Rodgers, *Chem. Phys. Lett.*, 1971, **9**, 107.
16 A. Tsuchida and M. Yamamoto, *J. Photochem. Photobiol., A*, 1992, **65**, 53.
17 A. Tsuchida, T. Ikawa, M. Yamamoto, A. Ishida and S. Takamuku, *J. Phys. Chem.*, 1995, **99**, 14 793.
18 C. Bohne, E. B. Abuin and J. C. Scaiano, *J. Am. Chem. Soc.*, 1990, **112**, 4226.
19 Y. Barenholz, T. Cohen, R. Korenstein and M. Ottolenghi, *Biophys. J.*, 1991, **60**, 110.
20 S. L. Murov, I. Carmichael and G. L. Hug, *Handbook of Photochemistry*, Marcel Dekker, New York, 2nd edn., 1992.
21 M. A. J. Rodgers, *J. Chem. Soc., Faraday Trans. 1*, 1972, **68**, 1278.
22 P. L. Piciulo and J. K. Thomas, *J. Chem. Phys.*, 1978, **68**, 3260.
23 M. Gratzel, K. Kalyanasundaram and J. K. Thomas, *J. Am. Chem. Soc.*, 1974, **96**, 7869.
24 Y. Mori, A. Yoneda, H. Shinoda and T. Kitagawa, *Chem. Phys. Lett.*, 1991, **183**, 584.
25 Kh. Grellman and A. R. Watkins, *J. Am. Chem. Soc.*, 1973, **95**, 983.
26 J. W. Steed and J. L. Atwood, *Supramolecular chemistry*, J. Wiley & Sons Ltd., West Sussex, UK, 2000.
27 T. Yorozu, M. Hoshino, M. Imamura and H. Shizuka, *J. Phys. Chem.*, 1982, **86**, 4422.
28 K. Kano, I. Takanoshita and T. Ogawa, *J. Phys. Chem.*, 1982, **86**, 1833.
29 K. Kano, I. Takenoshita and T. Ogawa, *Chem. Lett.*, 1980, 1035.
30 S. S. Atik and J. K. Thomas, *J. Am. Chem. Soc.*, 1981, **103**, 4367.
31 E. Blatt, A. Launikonis, A. W. H. Mau and W. H. F. Sasse, *Aust. J. Chem.*, 1987, **40**, 1.
32 E. Blatt, *Aust. J. Chem.*, 1987, **40**, 851.
33 K. Kano, H. Matsumoto, S. Hashimoto, M. Sisido and Y. Imanishi, *J. Am. Chem. Soc.*, 1985, **107**, 6117.
34 H. Kobashi, M. Takahashi, Y. Muramatsu and T. Morita, *Bull. Chem. Soc. Jpn.*, 1981, **54**, 2815.
35 A. Harada and S. Nozakura, *Polym. Bull. (Berlin)*, 1982, **8**, 141.
36 S. Hamai, *J. Phys. Chem.*, 1988, **92**, 6140.
37 Y. Yamamoto, S. Shiraki and Y. Kawamura, *J. Chem. Soc., Perkin Trans. 2*, 1992, 2241.
38 Y. Taniguch, Y. Nishina and N. Mataga, *Bull. Chem. Soc. Jpn.*, 1972, **45**, 2923.
39 H. M. Rosenstock, K. Draxl, B. W. Steiner and J. J. Herron, *J. Phys. Chem. Ref. Data*, 1977, 6, Supplement No. 1.
40 *CRC Handbook of Radiation Chemistry*, ed. Y. Tabata, Y. Ito and S. Tagawa, CRC Press, Boca Raton FL, 1991.
41 I. P. Bell, M. A. J. Rodgers and H. D. Burrows, *J. Chem. Soc., Faraday Trans. 1*, 1977, **73**, 315.
42 *Photoinduced Electron Transfer*, Elsevier, Amsterdam, 1988.
43 S. L. Mattes and S. Farid, *J. Am. Chem. Soc.*, 1986, **108**, 7356.
44 I. R. Gould, D. Ege, J. E. Moser and S. Farid, *J. Am. Chem. Soc.*, 1990, **112**, 4290.